APPENDIX 15

GENERAL GEOSCIENCE DATA PARAMETERS

Table of Contents

List of Tables

Table 15-1. Description of General Parameters for the Geoscience Data Sets

Geoscience Discipline	Task Leader	Raw Baseline Data	Data Source	Modeled Baseline Parameter
Gravity and Magnetics	Bob Karlin	Gravity and Density	Complete Bouguer anomaly gravity data PACES gravity data	Combined Gravity-Magnetic Modeling to infer Lithology
		Magnetics	HELIMAG aeromagnetic total field anomaly data Graugh (2002)	
		Horizontal Gradients	Blackwell et al. 2005	
Seismic	Ileana Tibuleac	Velocity Modeling	OPTIM interpreted velocity models General crustal-scale tomography	P-wave velocity S-wave velocity Attenuation Rho (density)
		Reflection Profiles	Available seismic profiles and interpreted lines	
Thermal	Dave Blackwell[1]	Temperature (°C)	surface measurements, temperature gradient holes and deep wells	Modeled Wellfield Temperatures Conductive Model Convective Model
		Thermal Gradients	temperature-depth profiles	
		Heat Flow	Blackwell and SMU Thermal Modeling	
		Thermal Conductivity		
Magnetotellurics (MT)	Phil Wannamaker	Resistivity	contiguous bi-pole deployments across three dense profiles (Arrays S, C and N) Wannamaker et al. 2006; 2007	Resistivity
Geo-chemistry	Mack Kennedy	Si, Cl and Total Bicarbonate (ppm) Bicarbonate-Cl (ratio) F[$_4$He] (ppm) Helium R/Ra CO_2 Geothermometry	surface (fumaroles, springs, shallow wells) and wells at depth (production fluids, etc.); compiled in Goff et al. 2002	None
Lithology	Trenton Cladouhos[2]	Lithology (surface and wells)	Geologic Maps and available well logs	Lithology Type Assigned Parameters:

Table 15-1. Description of General Parameters for the Geoscience Data Sets

Geoscience Discipline	Task Leader	Raw Baseline Data	Data Source	Modeled Baseline Parameter
				Density, Strength, Internal Friction
Stress	Trenton Cladouhos[3]	Coulomb Failure Stress	Stress Modeling: Caskey et al. 2000	Coulomb Stress Change Dilatation Fault Orientation Fracture Intensity Zones of Compression/Dilation
		Fault orientation/slip	Faulting Databases	
		Borehole stress data	Hickman et al. 1998; 2000	

[1]Supported by Mahesh Thakur of SMU

[2]Supported by Owen Callahan and Jon Sainsbury from AltaRock Inc.

[3]Supported by Maisie Nichols of AltaRock Inc.

Table 15-2. List of detailed Geoscience Parameters from the Dixie Valley baseline data set and associated applicability and resolution

Parameter	Type	Source	Description	Unit	Used in Statistical Analysis	Data Applicability	Resolution
LithDen	Assigned	Lithology	Density	g/cm^3	Y	N/A	N/A
LithStrength			Strength	Mpa	N		
LithInterFric			Internal Friction	N/A			
Rock Type	Measured/Modeled		Lithology Type	N/A	Y	at surface and at depth within wellfield	0.5 km
FracInten	Calculated	Stress	Fracture Intensity	m/m^2	Y	entire project area	0.5 km
VertStress			Vertical Stress	bars		entire project area	unknown
CSC	Modeled		Coulomb Stress Change	bars		wellfield only	
Dilatation			Dilational Strain	N/A			
Temperature	Measured/Modeled	Thermal	Temperature	° C	Y	Wellfield only	0.5 km
Vp	Modeled	Seismic	P-wave velocity	km/s	Y	Proximal to seismic reflection lines	0.5km
Vs			S-wave velocity	km/s			>10 km
Rho			Density	g/cm^3	N		
Qp			P-wave attenuation	-			
Qs			S-wave attenuation	-			
Resistivity	Modeled	MT	MT derived resistivity	ohm-m	Y	wellfield only	0.5 km
Si	Measured	Geochemistry	Silica	ppm	N	wellfield and other springs within project area	unknown
Cl			Chloride	ppm			
BiCarb			Total BiCarbonate	ppm			
BiCarb-Cl			BiCarb/Chloride	N/A			
F[$_4$He]			Fractionation of ^{4}He				
R/Ra			He^3/He^4 ratio	N/A			
Grav_Mag	Modeled	Gravity-Magnetics	Gravity-Magnetics inferred Lithology	N/A	Y	within wellfield	0.5 km

Other Potential Parameters							
Fault/Fracture Azimuth	Modeled	Geology-Stress	Favorable/Unfavorable Fault Orientations	degrees	N	entire project area	unknown
Compression-Dilation Zones	Modeled	Stress	Expected localized stress zones	N/A	N	major structural intersections	0.5 km
Gravity	Measured/Modeled	Gravity-Magnetics	gravity measurements	gals	N	entire project area	unknown
			density	g/cm^3			
Magnetics			magnetic susceptibility	emu/cm^3			
Horizontal Gradients			area of largest gradients infer major faulting	N/A		only at surface	
CO_2	Measured	Geochemistry	CO_2 Flux	g/m^2d	N	major structural intersections	<<500m

Table 15-3. Geologic and Thermal Cross-Sections Data Sources[3,4]

Type	Source	Inference	Baseline Conceptual Model Report	
			Figure Reference	Section/Appendix Reference
Surface Geology	Speed (1976) Map	geology and faulting in the Stillwater Range		Appendix 1
	GIS-referenced Dixie Valley Map	occurrence of stratigraphic units and major faults	51	Section 7.3
Well Data	Blackwell et. al. (2005)	available temperature and lithology at depth	40A, 42, 43, 46, Table 3	Section 6; Appendix 9, 10 and 11.
	Lithology logs[1] from Al Waibel[2]			
	SMU[5] & NBMG[6] databases			
Gravity / Magnetic Surveys	Blackwell et. al. (2005)	Horizontal gradients infer areas of intrabasinal faulting	8, 9, 10, 11 and 13	Section 3.1,3.2
		Location of piedmont structure		
Seismic Reflection Profiles	Blackwell et. al. (2005)	infer faulting and depth to prominent reflectors along interpreted profiles	17a	Section 3.5.3
DV Structure Map	Smith and Blackwell (2001)	Intra-basin structures	14	Section 3.2
DV Basement Configuration	Blackwell et. al. (2005)	Intra-basin structures, depth to basement	18	Section 3.5
		depth of basin-fill from drilling and seismic reflection profiles		
Cross-sections	Johnson and Hulen (2002)	northern producing field	47	Section 6.4
	Blackwell et. al. (2005)	conceptual geologic cross-sections		
	Blackwell et. al. (2005)	conceptual thermal sections	45A, 45B	Section 6.3
	Plank (2002)	Structure of the producing wellfield		

Table 15-3. Geologic and Thermal Cross-Sections Data Sources[3,4]

Type	Source	Inference	Baseline Conceptual Model Report	
			Figure Reference	Section/Appendix Reference

Note. Structural Map from Waibel (2011) and unpublished structure maps (Figures 49A-C) produced by Jon Sainsbury of AltaRock Inc. were not used to construct the cross-sections

[1]Lithology Logs for selected Dixie Valley Wells were provided by Al Waibel with the permission of Terra-Gen Power.

[2]Geothermal consultant and member of Project Peer Review committee

[3]A detailed description of all the assumptions used in the cross-sections can be found in Appendix 12.

[4]A total of eight cross-sections through the Dixie Valley Geothermal Wellfield area can be found in Appendix 12.

[5]Southern Methodist University

[5]Nevada Bureau of Mines and Geology

Table 15-4. Lithology Parameters

Major Recognized Lithologic Units

Lithcode	Description
Air	There is almost two kilometers of relief in the project area, so all cells above the surface are given the designation "air".
Q-Tbf	This represents all Tertiary to Quaternary valley-fill sediments above the Miocene Basalt (Tmb).
Tmb	Overlying the Mesozoic section are Tertiary volcanics, with the Miocene basalt being the thickest single unit in the Stillwater Range and under the valley. Therefore, the Tmb is considered the dominant mechanical unit in these locations. Further east in the Clan Alpine Range, the Oligocene tuffs are far thicker and may dominate there.
Kgr	Cretaceous and possibly early Tertiary granodiorite which outcrops at edges of ranges (west and east side of Stillwater Range, west side of Clan Alpine). Granite is reached in some boreholes below the valley-fill within the footwall block of encountered faults.
Jz	The Jurassic Aulacogen includes a variety of keratophyric intrusive rocks, mafic extrusives and some marine sediments such as the Boyer Ranch Quartzite. From a mechanical standpoint these are grouped into a single, strong unit.
Tr	Triassic sediments are varied, consisting of mostly meta-sediments including shales, limestones and phylites and considered to be the autochthon into which the Jurassic rocks were thrust into and over. A Paleozoic section is not included as it only occurs in NE corner of Project Area.

Lithology Dependent Assigned Parameters

LithCode	density	strength	internal friction	EGS Favorability (0-1)
Air	0	0	0	0
Q-Tbf	1.3	1	0.5	0
Tmb	2.5	100	0.7	0.6
Jz	2.6	400	0.8	0.7
Tr	2.4	30	0.6	0.4
Kgr	2.5	230	1.4	0.8

Notes:

LithCode represent the abbreviation for the lithologic unit that encompasses the majority of a given cell.
Density values are estimated from standard samples. TAMU results will allow for more precise measures.
Strength is uniaxial compressive strength (Mpa) for standard samples.
EGS Favorability of Rock is qualitatively assigned based on field excursion by Cladouhos and Callahan.
-- Other qualitative parameters considered include fracturing, rock strength, and variability of a litho-unit.

Other parameters

Value	Data Quality	Description
0	no lithology	no data
0.3	Soft	Geologic educated guesses, usually shown with question marks on geologic cross sections
0.5	Semi-soft	Determined from geologic cross sections, geologic inference, and stratigraphic column thickness
0.8	Medium Hard	includes seismic data, and projection from cells within 1 km.
1	Hard	Hard data includes surface outcrops, and well data. In a 500x500 m grid, this is not considered achievable due to variability of lithology in the grid block

Note: Generally the uncertainty is considered to vary smoothly and gradually. So that if one cell is Medium Hard (0.8), then the adjacent cells, which obtains information from the Medium hard cell would be 0.7.

Table 15-5. Well Statistics Parameters

This sheet explains all the parameters in reference to Dixie Valley wells. A data file with all the available well data including hard data (well logs, temperature profiles, geochemistry) and modeled data (Gravity, Magnetics, Seismic, MT) in reference to well location was compiled for use in a geostatistical analysis (see Appendix 16b). The geoscience data was gridded along depth slices every 0.5km starting at the surface, around 1km above sea level (asl) and ending at -3km asl. The trust (confidence) of the data is included where applicable, highlighted light orange, and used for the geostatistical analysis and EGS Favorability Mapping.

	Trust (Confidence) Value for the derived data in that specific cell (depth) ranging from 1 to 5.

Trust Value	Description
5	Hard Data (measured in wells)
4	Strongly Inferred Data, within 0.5km of hard data
3	Weakly Inferred Data, within 1km of hard data
2	Interpolated/Extrapolated Data, more than 1km from hard data point
1	No Data available

1. **Well:** The well name is as indicated and in reference to section number.
2. **Type:** Wells were divided into the following classes; Injector, Producer, Sub-Commercial, and Other. Other was used if the well type was unknown.
3. **Location:** X and Y are the coordinates of the well at the surface in latitude and longitude. Z is the elevation in meters at the surface (KB).
4. **Depth:** Well were divided into depth intervals from 1km asl (surface of Dixie Valley) to -3km asl in 0.5km increments.
5. **Lithology:** Well Lithology as reported in the literature, well logs, etc. that occurs at the identified horizontal slice (km above sea level). The following table divides the lithology into seven stratigraphic units.

Unit	Description
Tbf	Basin-filling sediments including lowermost tuffaceous sediments.
Tmb	Miocene basalt, aka Table Mountain Basalt.
Tv	Oligocene silicic volcanics, overlying lacustrine sediments, and underlying volcaniclastics.
Jbr	Jurassic Boyer Ranch quartzite
Jz	Jurassic Humboldt Igneous group
Tr	Triassic metasediments
Kgr	Cretaceous granodiorite

6. **Temperature: Measured** temperature in degrees Celsius extracted from the literature and Temp-Depth profiles (Blackwell et al., 2005).
7. **Modeled Temp:** Temperature in degree Celsius derived from the modeled temperature along the cross-sections.
8. **Vp-seismic:** P-wave velocity (km/sec) modeled at the University of Nevada Reno and derived from previous velocity modeling.
9. **MT:** Resistivity in ohm-m derived from Magneto-telluric data along three wellfield arrays (N,C,S).

*note. The MT data along Array C in the location of the Section 7 producing wells was applied to all the wells in this section.

10. **Grav_Mag:** Modeled Combined Gravity-Magnetic inferred lithology units

Unit	Description	Density (g/cm^3)	Magnetics (emu/cm^3)
Tbf	Basin-fill	2.445	-
Ja	Jurassic arenite	2.56	-
Jv	Jurassic volcanics (rhyolite)	2.47	-
Jg	Magnetized Jurassic mafic rocks	2.876	0.004
Tr/Kgr	Tr meta-seds and basement	2.88	-

11. **Stress Parameters:** stress parameters derived from an AltaRock Energy Inc. generated stress model of Dixie Valley using Coulomb 3.1 (see Appendix 13). ***CSC*** (Coulomb Stress Change) on a given fault/fracture due to slip constraints on a number of source faults. Positive CSC infers failure is promoted, while negative CSC values infer failure is inhibited. ***Dilation:*** expected dilatation on fault/fracture due to CSC and model constraints. Positive values infer fault is open (unclamped), while negative values (compression) infer fault is closed (clamped).
12. **VertStress:** Vertical Stress (bars) calculated based on the depth and density of overlying rocks.
13. **Productive (Hydrothermal):** 1 infers the referenced cell (depth) is capable of geothermal injection, production (permeable), or sub-commercial. 0 infers the cell (depth) is not hydrothermal.
14. **Faults Present:** Fault zones identified in the well logs (1 = fault present at the corresponding depth interval).

Table 15-6. Seismic Parameters

The baseline seismic parameters are derived from a University of Nevada Reno generated model that integrated the OPTIM velocity modeling results along the seismic reflection profiles with other regional studies and general crustal-scale tomography. Values were provided for pre-determined 500m by 500m cells up to a 5km depth within the Wellfield Calibration area and along key wellfield cross-sections lines. A "trust" factor was also included to give the SME opinion on the confidence in the model with a particular cell.

The seismic model includes 5 parameters:

1. Vp = P-wave velocity in km/s
2. Vs=S-wave velocity in km/s
3. Density (RHO) in g/cm2
4. P-wave Qp attenuation factor
5. S-wave Qs attenuation factor

"Trust" factor: Confidence of the Baseline Data

The trust factor is 0.9 for the models with highest resolution (Optim reflection lines) and 0.01 for the general models. Regional models are given a "trust" factor from 0.2 to 0.5.

Model derivation description

1. The models in Appendix 2, Tables 3 and 4 were used to create an integrated model for the study area.

2. We used algorithms written in Matlab. A set of depths of interest were chosen for all models. Each model was stored into a Matlab structure. Each structure includes the model reference, the model area (which is a square oriented North-South, East-West), and the parameter model.

3. The parameter model matrix consists of seven columns: depth, P velocity in km/s, S velocity in km/s, density (g/cm3), P and S attenuation factors Qp and Qs and a "trust" factor, described below. "No information" is marked by the parameter value set to -99.

4. The "trust" factor ranges from 0 to 1 and is, for example, set by the analyst up to 0.9 for the Optim reflection/refraction lines and is set to 0.01 for general and non-local models. Using the "trust" parameter, seismic lines and local data are given higher weights than the general model weights.

5. A "slack" factor for each model represents a chosen extension of the model area in all directions. The larger is the "slack" parameter, the smoother is the model. Because of their 25-50 km resolution, the UNR models have a 0.01 trust value.

How is a model at one location (lat, lon) extracted?

The user inputs the point coordinates and the code estimates a model for that point, with parameter value variations as a function of depth. To estimate the parameter values (for example Vp) at each point in space and at each depth, the program finds all the models which include the respective point. Next, it collects all the Vp values, together with their "trust" values at each depth. The resulting P-velocity at the respective point and depth is a "trust" parameter weighted mean, after the "-99" (no data) estimates are discarded. Sixty-four independent models and the UNR model are currently used for the integrated model, including all the information in the study area collected so far. Each parameter value is independently estimated, none of the parameter values are derived using an equation from the other parameter values.

Resolution

For the 0.5 km grid exercise,Vp has low-enough resolution precisely along the Optim lines, if the "slack" parameter is 0.005 (~0.5 km). The slack parameter, however, for the current "smoothed" models is 0.03 degrees. That means the "method" error is ~ 0.03 deg, which is actually larger than the grid size. The reason the "slack" was empirically chosen 0.03 is to extend the Optim models to points in the vicinity and to avoid as much as possible

having to use, due to lack of data, an unrealistic parameter value (belonging to a world-wide model). All the lines and the slices have been calculated using this code. Outside the lines, Vp has ~ 25 km resolution. Vs has ~ 25-50 km resolution, and so do all the other variables.

Seismic Parameter	Description
Vp	derived from Optim model (Anonymous, 1998) reflection lines (highest resolution of around 0.5 km)
Rho	calculated from general earth model, regional studies (Abbott and Karlin) and independent of measured rock densities
Vs	uses a determined ratio factor of 1.6 for relationship with Vp, general earth model (low res.)
Qp, Qs	based on general relationships (very low resolution)

Table 15-7. Joint Gravity and Magnetics Modeling

Summary

The complete Bouguer anomaly gravity data, PACES gravity data and the HELIMAG aeromagnetic total field anomaly data were jointly modeled in along five lines labeled A-A' to F-F' in the geothermal area to create a 2 ½ D geophysical model consistent with the surface geology and well data. Lines C-C' through F-F' are perpendicular to the strike of the Stillwater Range and the Dixie Valley range-bounding fault. Lines A-A' and B-B' are parallel to the range. It was not possible to model the magnetics of the range- parallel line B-B' because of 3-D effects due to the extensive Jurassic section exposed in the southeastern part of the range.

Method

Gravity modeling was done using the GM-Sys module of the Oasis Montaj program from Geosoft Inc. Measured gravity models of unknown shape were forward modeled by trial and error adjustment of density and polygon vertices. Once the fit was considered close, XZ positions were optimized using inverse methods. The objective was to minimize the RMS error between observed and computed values. A fit was considered acceptable if the misfit F was less than 1% (F=100*RMS error/profile gravity data range). As described in the GM-Sys manual, 2-D models may be visualized as a number of tabular prisms with their axes perpendicular to the profile; blocks and surfaces are presumed to extend to infinity in the strike direction. 2¾-D modeling, as implemented in GM-SYS, allows the prisms to be truncated at some distance in the plus and minus strike directions (± Y). It also allows the strike direction to be skewed relative to the profile azimuth. The methods used to calculate the gravity and magnetic model response are based on the methods of Talwani et al., 1959, and Talwani and Heirtzler, 1964, and make use of the algorithms described in Won and Bevis, 1987. Two-and-a-half dimensional calculations are based on Rasmussen and Pedersen, 1979. The GM-SYS inversion routine utilizes a Marqardt inversion algorithm to linearize and invert the calculations (Marqardt, 1963). Gravity and magnetics models are non-unique, i.e., several model families can be created to match the data. It is up to the interpreter to assess whether the model(s) are geologically reasonable.

Model Parameters and Constraints

Basin-fill Density

1. Density contrasts, not absolute values are what control the gravity signature
2. Available well lithologies that defined the known basin depth were used to test densities for the basin-fill
3. The final basin fill density of 2.445 gm/cc was selected based on fitting the model to the observed basin fill depth in well 62-21 on line E-E'. Independent fits of lines D-D' and F-F' show basin fill depth are consistent with other wells in the area.
4. In some of the lines, it was necessary to introduce a surficial (<100 m) low density layer of D ~1.5-1.8 gm/cc to account for very short wavelength gravity variations. Likely representing the vadose zone or alternatively, lake and playa sediments.

Bedrock Density

1. Determined by modeling the outcropping bedrock on the eastern flank of the Stillwater Range which include Jurassic gabbros, Jurassic volcanics, and Triassic sediments.
2. A density of D=2.876 gm/cc. was found to provide the optimal fit to the slope of the CBA, and this value, which is typical of mafic volcanic rock was adopted for the rest of the lines.
3. A slightly reduced density of 2.4 to 2.5 gm/cc was proven necessary to model some near surface rocks in the Stillwater Range that are classified as rhyolites or mixed clay/limestone/arenites.

Regional Trend

1. Effects of removing a slight NW/SE regional trend was tested on the gravity models
2. The net effect was to slightly deepen the basins, but no significant changes were observed to the locations of the basin walls or the positions of postulated faulting.

Magnetization

1. Models with magnetizations of M=0.003 to M= 0.005 emu/cc yielded acceptable fits.
2. Positively magnetized units were assumed in the modeling due to the signature of rocks in the Stillwater Range that required positively magnetized bodies, prominent subsurface anomalies (positive highs) implying buried normally magnetized bodies, and the dominant positive magnetic field during the Jurassic.
3. Ambient field directions of inclination = 64° and declination = 0 were used in the modeling.
4. Susceptibility rather than remanence controls the magnetization.
5. A value of M=0.004 emu/cc was found to be optimal in modeling the magnetic signature of the Jurassic volcanics in all of the profiles.
6. The magnetic anomaly data can be successfully modeled with a single magnetic Jurassic mafic rock unit. The magnetic modeling is very sensitive to the shape and location of the individual blocks as well as the interaction between blocks.

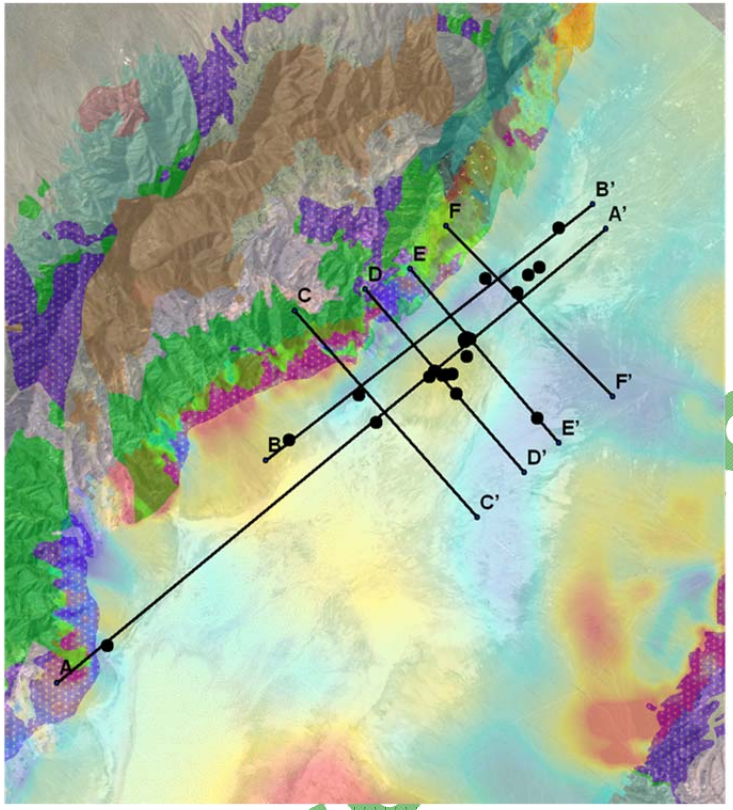

Location of modeled lines A-A' through F-F'' superimposed on the HELIMAG total magnetic field anomaly, the state geologic map and a satellite terrain map. Black dot are locations of geothermal wells. Purple and deep red colors are Jurassic gabbroic rocks (Jg), green colors area are Jurassic mafic volcanics (Jvb), and brown colors are Cenozoic volcanics, mostly basalts. Modeled Lines E and F are shown below.

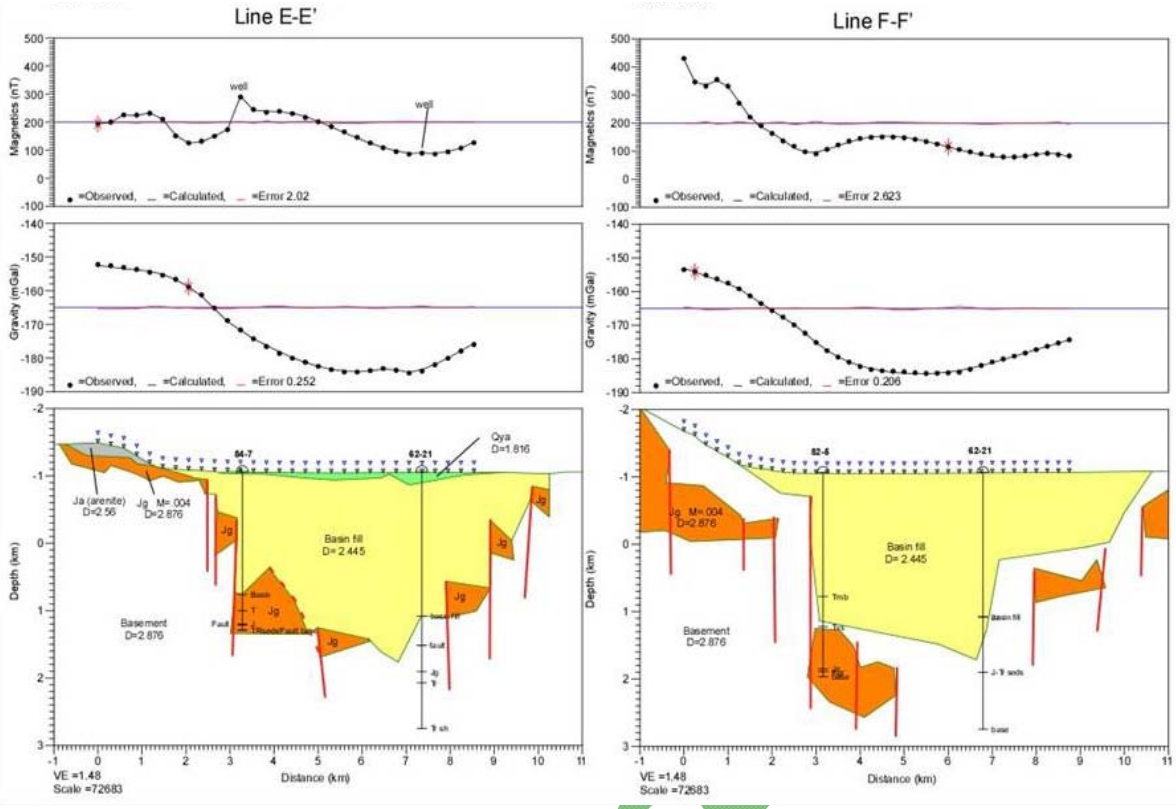

Joint gravity and magnetic model of lines E-E' and F-F'. Fits of gravity and magnetic profiles are <1%. Postulated faults are shown in red. Surfaces are basin fill (yellow, D=2.445 gm/cc); Jurassic mafic volcanics (orange, D=2.876 gm/cc, M=0.004 emu/cc); basement (white, D=2.876 gm/cc, M=0 emu/cc); lower density arenites or rhyolites (grey, D=~2.5 gm/cc, M=0 emu/cc).

Table 15-8. Magnetotellurics (MT) Modeling

A new generation MT-array system has been applied to three profiles over the Dixie Valley thermal area (see figure below). This study described in Wannamaker et al. (2007) is defined as state-of-the-art MT array measurements in contiguous bipole deployments across the Dixie Valley thermal area that have been integrated with regional MT transect data and other evidence. The modeling techniques can resolve the resistivity along the 2-D profiles at depth. Three profiles (N, C, and S) extend through the geothermal system, correlate geographically with the wellfield cross-sections and were used to quantitatively and quantitatively compare with the other geoscience data. The purpose of the MT survey in Dixie Valley was to (1) resolve the complex structural setting, (2) delineate fault zones which have experience fluid flux as indicated by low resistivity, (3) infer ultimate heat and fluid sources for the thermal area, and (4) investigate the capability of well-sampled electrical data for resolving subsurface structure.

Parameters

1. Contiguous bipole deployments across three arrays (N, C, and S).
2. Inversion techniques allow for higher resolution and account for 3-D effects.
3. Stand-alone MT soundings at one or both ends for local background control
4. Additional five-channel MT soundings to the SE end of each profile for improved aperture.
5. Array C integrated with regional transect data has a resolution to 10km (depth)

Array N

1. Derived from 60 array MT sites taken with contiguous E-field bipoles
2. Three stand-alone MT sites at the SE end.
3. Resolution to 4km depth
4. Extends through the northern producing area, 38-32 and Senator Fumaroles.

Array S

1. Dense MT array line plus three stand-alone MT sites to the SE.
2. Resolution to 4km depth
3. Extends through the hot and dry wells in the DVPP

Array C

1. 120 dense MT array measurements and 13 appended wideband MT sounding
2. Integrated with regional transect data
3. Resolution to 10km depth
4. Extends through the main producing area and 62-21 in the valley

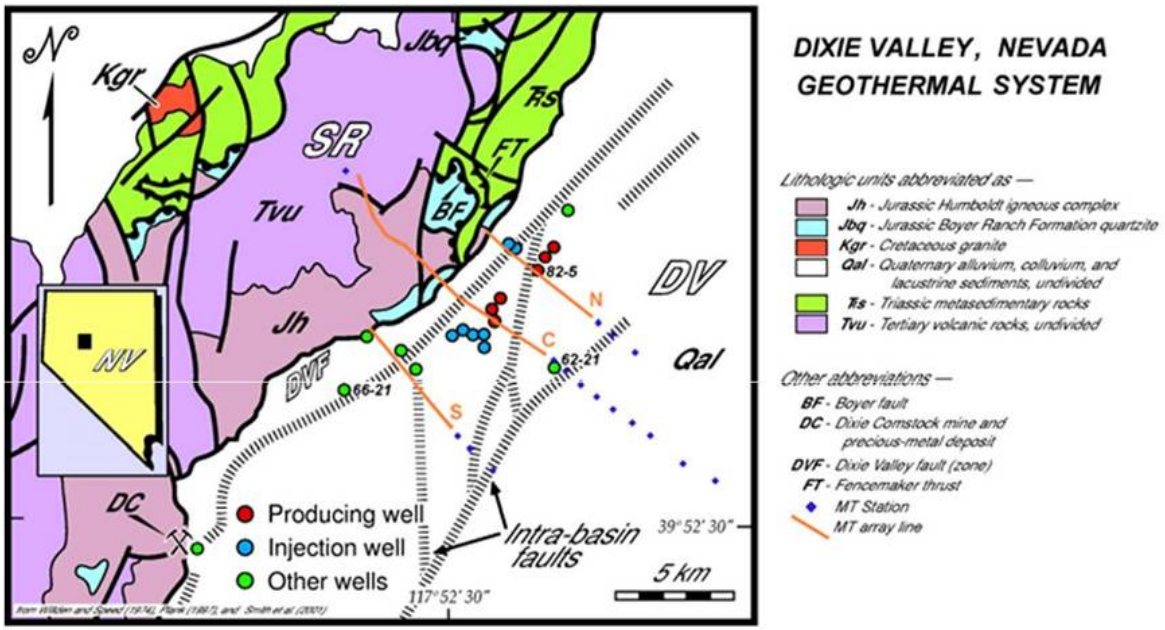

Simplified geologic map of the Dixie Valley (DV)-Stillwater Range (SR) area surrounding the Dixie Valley thermal field. Orange-brown lines are the MT profiles lines (see text) Lines are labeled N (north), C (central), and S (southern). Blue diamonds are five-channel MT stations added to extend profiles across the valley. Original figure courtesy of Jeff Hulen.

Table 15-9. Thermal Modeling

Thermal Models are shown as 50°C isocontours included on the major cross-sections (Appendix 12). A detailed description of assumptions used within the thermal cross-sections can also be found in Appendix 12. Using the thermal cross-sections and well data, an AltaRock thermal model was generated in the Wellfield Calibration Area in order the construct the EGS Favorability Maps. This model was derived from the well data, thermal cross-sections, and interpolations between the cross-sectional data.

Parameters

1. Modeled in degrees Celsius with 50°C contours from 100°C to 250°C
2. Used temperature measurements in available wells, temperature gradient holes (TGH) and fumaroles
3. Extracted temperature in incremental depths from T-D curves
4. General convective trend and extrapolated thermal conditions away from the wells were based on unpublished conceptual geothermal sections from Blackwell.
5. Assumes the range-bounding and piedmont faults are the main thermal-bearing structures in the DVFZ.
6. No temperature data beneath the Stillwater Range
7. Temperatures within Dixie Valley away from the DVFZ are poorly constrained

Cross-Sections

The table below shows the thermal data available per cross-section.

Section	Orientation	Fumarole	TGH	Well[1]
A-A'	SW-NE			**45-14**, **62-23A**, SWL-3, 74-7, **82-5**, **45-33**
B-B'	SW-NE			**66-21**, **36-14**, 45-5, **38-32**, **45-33**, **76-28**
C-C'	NW-SE	X	H-1	53-15, **36-14**, **62-23A**
D-D'	NW-SE			SWL-2, **52-18**, 65-18
E-E'	NW-SE			74-7, 76-7, **62-21**[2]
F-F'	NW-SE	X		**38-32**, 45-5, **82-5**
G-G'	NW-SE		SR-3	38-32, 37-33, 28-33
H-H'	NW-SE			**76-28**

1. Bolded wells have a T-D curve extracted from Blackwell et. al. (2005).
2. 62-21 was used to constrain temperatures in Dixie Valley for D-D' and F-F'.

Gridded Mapview Model

The expected temperature of the Wellfield Calibration Area at 12 different depths (1.5km to -4km above sea level at 0.5km increments) was modeled based on the available well data (hard measurements), thermal modeling along cross-sections (inferred) and interpolated temperatures between the modeled section lines. The thermal data was coded based on the type of data. Areas of elevated temperatures occur along the range-front fault at depth (36-14) and along the piedmont structure, consistent with recent interpretations of the thermal regime. The major constraint to the model is the lack of actual temperature measurements away from the wellfield and the reliance on inferred and interpolated data. Regardless, the Wellfield Calibration Area is the only portion of the EGS Study Area where any thermal data at depth is available.

Temperature-Depth Curves

1. T-D curves available for the following wells: 52-18, 62-21, 45-14, 66-21, 62-23A, 36-14, 76-28, 38-32, 82-5 and 45-33.
2. T-D curves represent equilibrium conditions except in 36-14, 66-21 and 45-14.
3. 66-21 and 45-14 have weak artesian flow.
4. 36-14 data below 2600m were derived from Horner-type extrapolations at a series of different BH depths, while at shallower depths the curve is based on more suspect extrapolations, as the upper portion of well was quite far from thermal equilibrium.

Table 15-10. Coulomb Stress Modeling

Overview
Coulomb 3.1 can calculate strain and Coulomb Stress Change (CSC) on a receiver fault (RF) due to the differing slip on a number of source faults (SF) in order to determine whether failure on the RF is promoted or inhibited. The program assigns the RF a specified strike, dip and rake and assumes that the RF exists within each grid cell. Coulomb then calculates and plots the strain or CSC value at that location. A first test, referred to as Scenario 1, reproduced the model from Wesnousky et. al. (2003) that broke up the slip into three sections based on Holocene ruptures namely, slip along the Dixie Valley Fault (1954), slip along the Pleasant Valley Fault (1915) and the lack any slip within the Stillwater Seismic Gap. This model assumes only a single range-bounding fault with a moderate dip (see figure 7 of main report).

Modeled Parameters
Coulomb Stress Change (CSC): The expected change in stress (+/-) on a receiver fault (3 options) in a given cell due to slip constraints on a number of pre-determined source faults.
Dilatation: The expected dilatational strain on a receiver fault (3 options) in a given cell due to slip constraints on a number of predetermined source faults.

Scenario 1
This first scenario replicated the stress analysis from Caskey et al. (2000) study using the same slip constraints.

Scenario 2
This second scenario builds on the replicated model (Scenario 1) and assumes that the whole Stillwater Seismic Gap (SSG) did rupture in the "Gap" earthquake. It also takes into account other significant structures such as piedmont faults, north-trending faults and other intrabasin structures. The Dixie Valley Fault (DVF) is still one section as is the Pleasant Valley Fault (PVF), while the SSG is broken up into three sections with different orientations and slip constraints. The three explored types of receiver faults (RF) are (a) a synthetic normal fault subparallel to SGS dipping 70oE, (b) antithetic normal fault subparallel to SGS dipping 70oW, and (c) normal fault oriented roughly N-S dipping 70°W.

Slip Parameters

- 1915 Pleasant Valley Earthquake along PVF
  - Max vertical/horizontal displacements are **5.8m**/**2m**, respectively (Wallace, 1980; 1984)
  - Dip varies from **47-65° NW** (QFFDB)
- 2-2.5 ka "Gap" Earthquake along SGS
  - Max vertical displacement of 5m (Caskey and Ramelli, 2004)
  - Dips to the SE, but no angle reported by QFFDB; Blackwell et al. (2005) suggest dips 70-80° SE down to at least 3km
- *1954 Dixie Valley Earthquake along DVF*
  - Max vertical displacement of **2.8m** (Caskey et al., 1996)
  - Dip varies from **30-80° SE** (QFFDB)

Summary of Model
A program called Coulomb 3.1 (http://earthquake.usgs.gov/research/modeling/coulomb/) was used to calculate strain and stress changes on receiver faults caused by slip on source faults in the region surrounding the Dixie Valley Geothermal Field (DVGF). Source faults of interest in DV include the 2-2.5 ka Stillwater Seismic Gap (modeled here as 3 segments), the 1915 Pleasant Valley Fault, and the 1954 Dixie Valley Fault.

Receiver faults of interest are normal faults synthetic to the SSG (Syn_70E), antithetic to the SGS (Anti_70W), and oriented roughly N-S (N-S_70W). Coulomb 3.1 resolves the strain and stress changes caused by slip on the source faults onto a specified receiver fault in each grid cell. For each of the 3 receiver faults, we have 2 output files ("strain_xx.cou" & "dcff_xx.cou") at 11 depth slices (from 0.0 - 5.0 km, w/0.5 km spacing), for a total of 66 output files (Excel-compatible). Depths are given within the filenames, i.e. "strain_3.5.cou" contains strain values at 3.5 km depth. Note that our depth datum is roughly the average elevation of surface faults in Dixie Valley, or ~1100 m (+/- 100 m).

Model Boundaries and Grid Parameters

Model boundaries:

min. lat = 39.3300000
max. lat = 40.6800000
min. lon = -118.3300000
max. lon = -117.4000000
zero lat = 39.3300000
zero lon = -118.3300000
(ORIGIN = zero lat, zero lon)

Grid Parameters (in km):

Start-x = 0.0000000
Start-y = 0.0000000
Finish-x = 79.2114774
Finish-y = 150.1131510
x-increment = 0.5000000
y-increment = 0.5000000

Output Data Files

Strain Output

1	2	3	4	5	6	7	8	9	10
x	y	z	exx	eyy	ezz	eyz	exz	exy	dilatation

1. The first 3 columns are the x, y, and z coordinates of the gridpoint (km from origin).
2. The next 3 are the principal strain values (extension is +).
3. The next 3 are the shear strain values (right-lateral is +).
4. The last column is the dilatational strain value (dilatation is +).

Coulomb Stress Change (CSC) Output

The dcff_xx.cou files "dcff" stands for change in Coulomb Failure Function $\Delta\sigma f = \Delta ts + \mu' \Delta\sigma n$, where: $\Delta\sigma f$ = change in Coulomb failure stress; Δts = change in shear stress; μ' = effective coefficient of friction on fault; and $\Delta\sigma n$ = change in normal stress) contain 6 columns:

1	2	3	4	5	6
x (km)	y (km)	Z (km)	Coulomb (bar)	Shear (bar)	Normal (bar)

1. The first 3 columns above are the x, y, and z coordinates of the gridpoint (km from origin).
2. The last 3 columns above are the Coulomb failure stress change (+ promotes failure), shear stress change (right-lateral is +), and normal stress change (unclamping fault is +)

Table 15-11. Geochemistry

Geochemical data was provided by Mack Kennedy of Lawrence Berkeley National Laboratory (LBNL) and derived mostly from the comprehensive geochemistry database within Goff et al. (2002). The data was provided along the gridded cross-sections A through F where the occurrence of deep wells, temperature gradient holes, fumaroles, and springs coincided with the cross-section lines. The data was placed in a 500m by 500m cell and depths were estimated based on SME. Only parameters that were considered potential geothermal indicators were provided. These parameters are listed below. Due to the limited data and point source nature, this data was analyzed, included in the baseline database, but was not used in the formulation of EGS Favorability Maps.

Parameters	Description
Si	Silica (ppm)
Cl	Chloride (ppm)
Bi-Carb-Cl	Ratio of Bicarbonate to Chloride
F[^{4}He]	Fractionation of Helium (ppm)
R/Ra	Ratio of ^{3}He/^{4}He

Example of gridded geochemical data for silica (ppm) along Cross-Section B-B"